Inorganic Chemistry
Article
pubs.acs.org/IC

Structural Dynamism and Controlled Chemical Blocking/Unblocking of Active Coordination Space of a Soft Porous Crystal

Abhijeet K. Chaudhari, Sanjog S. Nagarkar, Biplab Joarder, Soumya Mukherjee, and Sujit K. Ghosh*

Indian Institute of Science Education and Research, Dr. Homi Bhabha Road, Pashan, Pune 411008, India.

Ⓢ *Supporting Information*

ABSTRACT: A three-dimensional biporous soft porous coordination polymer containing active coordination space, made of cadmium(II) and a tripodal carboxylate ligand bearing ether linkages, was synthesized and characterized. Guest-dependent dynamic activities in the active coordination space of the soft porous crystal have been explored. We have demonstrated controlled chemical blocking and unblocking of active pores of the dynamic framework along with guest-dependent contraction and expansion of the channels by single-crystal-to-single-crystal structural transformation studies. Detailed studies revealed up to 70% contraction of the void volume and almost a 100 times increase in gas sorption by controlled phases obtained by guest switching. These types of soft materials with porous scaffolds, also known as soft porous crystals, may have general implications in the preparation of intelligent host materials with zeolitic properties and enzyme-like specificity.

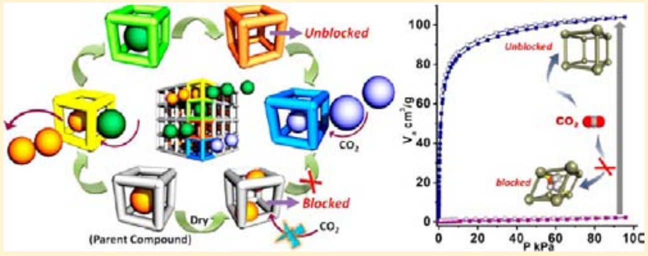

INTRODUCTION

Porous coordination polymers (PCPs) or metal–organic frameworks in recent times have attracted significant attention and emerged with a variety of possible designs for making tailored topologies and pore metrics.[1−3] One of the important features of PCPs is their regular long-range integrity bearing porous channels that can be utilized for potential applications such as gas storage,[4−7] chemical separation,[8−10] heterogeneous catalysis,[11−14] sensing,[15−19] conductivity,[20,21] chiral separation,[22,23] drug delivery,[24] etc. In this realm, the chemical versatility of the metal ions and organic linkers that constitute the PCPs allows various kinds of unique characteristic structural behaviors and host–guest activities.[25] Crystalline frameworks, which are soft in nature and possess flexibility in the host (soft porous crystals), are relatively less studied with respect to their structure–property correlations because of the difficulties of postmodification structural characterization.[26] Because of their structural dynamism and highly ordered network, these types of soft materials also exist as bistable or multistable forms by virtue of bond breaking/making, ligand substitution, guest exchange, etc.[26,27] Framework dynamism of PCPs is being considered as one important approach to modulate various physical properties like magnetism,[28] nonlinear optics,[29] sensing,[30] storage,[31] and several other porous properties.[32] Especially, after structural alteration of the channels and cavities of the soft PCPs, it may interact very differently with the guest molecules to provide unique porous characteristics.

To attain softness in PCPs, the use of an organic linker with flexible points can be a straightforward strategy, which can be further improved by the use of metal ions with variable coordination geometry. Cooperative actions of the soft inorganic backbone containing metal ions with variable coordination geometry capable of ligand substitution at the metal center[33] and organic linkers with flexible points[34] may offer interesting phenomena inside the coordination space of PCPs to develop novel functional activities of porous materials. The use of organic ligands with ether linkages as flexible points (which also provide reasonable rigidity) can facilitate structural changes of dynamic frameworks. On the other hand, cadmium(II) generally forms frameworks with a coordination number of 7 (most of the times, with one coordinated solvent) but also is stable with a coordination number of 6 and behaves as a soft flexible inorganic backbone. Taking advantages of the above facts, herein we report guest-dependent structural dynamism of a three-dimensional (3D) biporous PCP, containing active coordination space, made of cadmium(II) and a tripodal carboxylate ligand bearing ether linkages. Controlled chemical blocking and unblocking of the active pores of the dynamic framework along with guest-dependent contraction and expansion of the channels have been observed by single-crystal-to-single-crystal (SCSC) structural transformations, facilitated by the cooperative effects of flexibility of the linkers and softness of the inorganic backbone. Along with crystallographic studies of different phases with as much as 70% contraction of the void volume, dynamic activities within the active coordination space of the framework are also supported by almost a 100 times increase in carbon dioxide sorption by a new porous phase obtained by guest switching compared with the air-dried phase of the as-synthesized compound.

Received: August 9, 2013
Published: October 16, 2013

ACS Publications © 2013 American Chemical Society

dx.doi.org/10.1021/ic402058f | *Inorg. Chem.* 2013, 52, 12784−12789

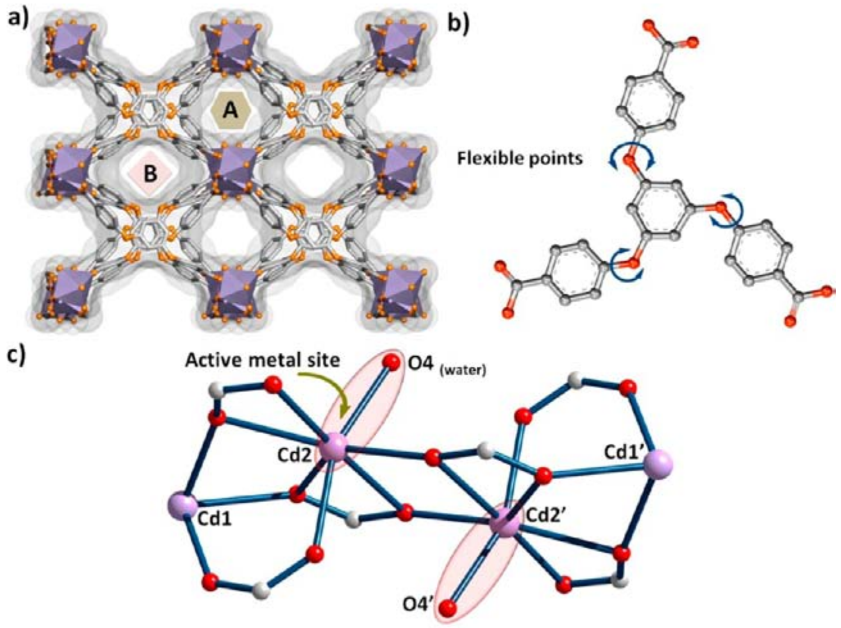

Figure 1. (a) Compound **1** with two types of channels, A and B, (b) an organic linker (**L**) with flexible points, and (c) the coordination environment of **1** with the active metal site.

■ EXPERIMENTAL SECTION

General Methods. All chemicals and solvents were commercially available and were used without further purification. Thermogravimetric analysis (TGA) was performed using a Perkin-Elmer STA 6000 simultaneous thermal analyzer; all samples were heated from 30 to 500 °C at a rate of 10 °C/min. The powder X-ray diffraction (PXRD) patterns were measured using a Bruker D8 Advance in the range of $2\theta = 5-40°$ with a scan rate of 0.5°/min. Solid-state UV measurements were recorded using a Perkin-Elmer Lambda 950 UV/vis spectrometer. Solid-state luminescence was measured using a Horiba Jobin Yvon Fluorolog-3 spectrofluorometer. Fourier transform infrared (FT-IR) spectra were measured in Nicolet 6700 FT-IR spectrometer using a solid sample containing KBr pellets. All samples were exposed to air before and during X-ray diffraction data collection. PXRD and TGA were used to identify the phase purity of the product and the structural dynamics in the solid state.

Synthesis of Compound $\{[Cd_{1.5}(L)(H_2O)]\cdot 2THF\}_n$ (1⊃THF). Ligand 4,4′,4″-(benzene-1,3,5-triyltrimethylene)tribenzoic acid (H_3L) (0.075 mM, 36 mg) was deprotonated in aqueous solution using NaOH, and the solution pH was maintained at about 6.2–6.6. Then the aqueous solution of $Cd(NO_3)_2\cdot 4H_2O$ (0.05 mM, 15.42 mg) was slowly added in the ligand solution. The total volume of the mixture was maintained at 4 mL using water as the solvent. Further tetrahydrofuran (THF) was added (2 mL) as a second solvent in the reaction mixture. This reaction mixture was allowed to react in a Teflon vessel (of capacity 18 mL volume) sealed in a steel vessel at 160 °C for 3 days. The reaction was allowed to cool slowly at a rate of 5.5 °C/h. After slow cooling of the reaction mixture, it yielded colorless block-shaped fully grown clean crystals of **1⊃THF**. Anal. Calcd for $C_{70}H_{70}Cd_3O_{24}$: C, 51.50; H, 4.32. Found: C, 51.46; H, 4.36.

Synthesis of Compound $\{[Cd_{1.5}(L)(H_2O)]\cdot 2ACTN\}_n$ (1⊃ACTN). Compound **1⊃ACTN** (ACTN–acetone) was made from **1⊃THF** by keeping crystals of **1⊃THF** in the acetone solvent for 3 or 4 days. After 3 or 4 days, a completely transformed compound **1⊃ACTN** was obtained. Anal. Calcd for $C_{54}H_{38}Cd_3O_{20}$: C, 48.25; H, 2.85. Found: C, 47.82; H, 3.12.

Synthesis of Compound $\{[Cd_{1.5}(L)(BuOH)]\cdot THF\}_n$ (1⊃BuOH). This compound also made by following the same procedure as that used for making compound **1⊃ACTN** except that 1-butan-1-ol (BuOH) was used in place of acetone (ACTN). Anal. Calcd for $C_{70}H_{64}Cd_3O_{20}$: C, 53.81; H, 4.13. Found: C, 53.92; H, 4.21.

Synthesis of Compound $\{[Cd_3(L)_2(H_2O)(THF)]\cdot 2THF\}_n$ (1D). Compound **1D** was obtained just by keeping the crystals of compound **1⊃THF** at room temperature and allowing them to dry for 1 h. Anal. Calcd for $C_{66}H_{56}Cd_3O_{22}$: C, 51.53; H, 3.67. Found: C, 51.12; H, 4.12.

X-ray Crystal Structure Determinations. Single-crystal X-ray data for all crystals were collected at 200 K on a Bruker Kappa APEX II CCD duo diffractometer (operated at 1500 W power, 50 kV, 30 mA) using graphite-monochromated Mo Kα radiation (λ = 0.71073 Å). The crystals were on nylon CryoLoops (Hampton Research) with Paratone-N (Hampton Research). The data integration and reduction were processed with *SAINT*[35] software. A multiscan absorption correction was applied to the collected reflections. The structure was solved by direct methods using *SHELXTL*[36] and was refined on F^2 by a full-matrix least-squares technique using the *SHELXL-97*[37] program package within the *WINGX*[38] program. All non-hydrogen atoms were refined anisotropically. The structures were examined using the *Adsym* subroutine of *PLATON*[39] to ensure that no additional symmetry could be applied to the models.

■ RESULT AND DISCUSSION

A solvothermal reaction between $Cd(NO_3)_2\cdot 4H_2O$ and H_3L in THF/water (1:2, v/v) produced colorless crystals of **1⊃THF** (Figure 1).

Structural analysis by single-crystal X-ray diffraction (SC-XRD) showed that the 3D biporous framework is arranged like a square-grid network of stacked layers comprising metal–ligand units, with metal carboxylate chains extended along the *c* axis leaving porous channels along the same axis. Compound **1⊃THF** crystallized in a centrosymmetric monoclinic *C*2/*c* space group. It was observed that the formula unit of the compound contained two types of cadmium(II) centers along with a completely deprotonated tricarboxylate ligand. Along with the carboxylate ligand, one water molecule also coordinated to the Cd2 site, which is the labile site and easily exchangeable with other incoming coordinating guests. Carboxylate ligand **L** is coordinated to the metal centers in three different bridging modes, viz., μ^2-η^2:η^1, μ^3-η^1:η^2:η^1, and μ^2-η^1:η^1, satisfying an octahedral coordination environment around Cd1 and a seven-coordinated distorted pentagonalbipyramid environment around Cd2 (Figure 1c). Importantly, two types of channels are present within the structure having different shape and sizes; one is square-shaped with dimensions of ~4.7 × 4.1 $Å^2$ (excluding van der Waals radii), while another one is of hexagonal shape (~5.2 × 4.1 $Å^2$). This biporous framework consists of coordinated water molecules protruding into one of the channels (in channel A), while another channel is lined with hydrophobic surfaces of aromatic rings and an ether-linking moiety. Both channels are filled with THF guest molecules. THF molecules lead to strong hydrogen bonding with the coordinated water molecules with a minimum O_{water}---H_{THF} distance of 1.979 Å. The Cd2 center acts as an active metal site having a coordinated water molecule with a Cd−O distance of 2.263 Å. *PLATON* analysis of the compound showed a potential solvent-accessible void volume of 3367.0 $Å^3$, i.e., 36.1% per unit cell.

The use of organic tricarboxylic acid (H_3**L**) possessing free rotating arms as ether linkages between the rigid central benzene ring and Ar−COOH moiety facilitates the dynamic behavior of the framework (Figure 1). Because of the highly fragile nature of single crystals, monitoring the solid-state structural changes is very difficult. Here we were successfully able to show the effects of guest interaction with the dynamic framework by solid-state SCSC structural studies. Moreover, in situ smooth aqua exchange at the Cd2 center was driven by the THF guest molecules present inside the pores of the framework. The presence of flexible points in the organic moiety provides simultaneous cooperative actions during changes in the coordination environment of the active metal site, which leads to contraction and expansion of channels of the dynamic framework. The functional coordination space inside the framework is very sensitive to different types of guests either coordinating or noncoordinating in nature. Coordinating guests with suitable size can be easily accommodated within the pore, which interestingly interacts inside the pore, replacing (partially or completely) the coordinated water molecules from the Cd2 center. Various effects observed by different guest molecules on the pore dimensions of the framework resulting in solid-state structural changes are represented in a schematic fashion (Scheme 1 and Table 1). As an effect of structural changes mediated by THF coordination (when crystals were kept in room temperature out of the mother liquor, i.e., in dry form) to the metal center, a complete blocking of the pores was observed. Complete exchange of water by THF guest was not complete but partial at room temperature, leaving behind a framework with one coordinated water and one coordinated THF molecule in the formula unit, which changed to $\{[Cd_3(L)_2(H_2O)(THF)]\cdot THF\}_n$ (**1D**) from the parent compound (**1⊃THF**). In compound **1D**, three different cadmium centers are present, where the third metal center Cd3 has coordinated THF (Cd3---$O10_{THF}$ = 2.310 Å) in place of water, unlike the parent compound (Figure 2). Overall the framework pattern is the same in **1D** structure but importantly the coordination space inside the framework shrank with a decrease in the total solvent-accessible volume to 22.2% per unit cell. This suggests shrinking of the coordination volume by almost 40% per unit cell compared to the parent compound when it changes to **1D**. Compound **1D** also has free guest THF molecules inside the channels, which leads to strong hydrogen bonding with the coordinated water molecules (O_{THF}---O_{water} = 2.553 Å; Figure 2). After taking crystals out of the mother liquor, pore A gets completely blocked due to THF coordination at the metal center. This subsequently also affects the dimensions of pore B, as a result of it squeezing pore metrics. Here we showed two-way modulation of the framework porosity via guest-dependent blocking/unblocking of the coordination space. Thus, replacing the parent guest molecules with a weakly/noncoordinating guest, i.e., ACTN (acetone), revealed interesting results. ACTN molecules are easily removed from the framework with little changes in the pore dimensions of both pores in compound **1⊃ACTN** (**1⊃THF** after exchanging with ACTN). Thus, **1⊃ACTN** has less susceptibility toward the dimensional changes of pores A and B. In this case, the total potential solvent-accessible volume was found to be the 31.0% per unit cell, which signifies that the coordination space can be maintained with the least decrease in volume (14% per unit cell). The strongest guest impact was observed from the rigid guest THF after coordination to the cadmium(II) center, and the least dimensional change was observed in the case of

Scheme 1. Schematic Drawing Representing the Structural Parameter Changes in Pore A of the Different Compounds in Table 1

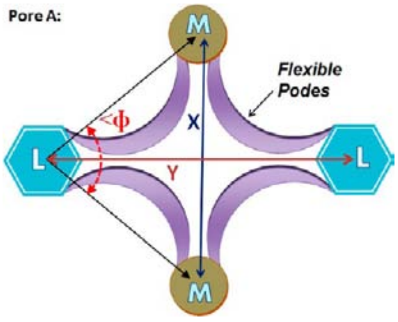

Table 1. Pore Dimension Changes in the Form of Three Parameters for Scheme 1

compound	∠ϕ (deg)	X (Å)	Y (Å)
1⊃THF	82.92	11.439	12.924
1⊃BuOH	80.14	11.075	13.160
1⊃ACTN	76.83	10.616	13.388
1D	74.81	10.251	13.588

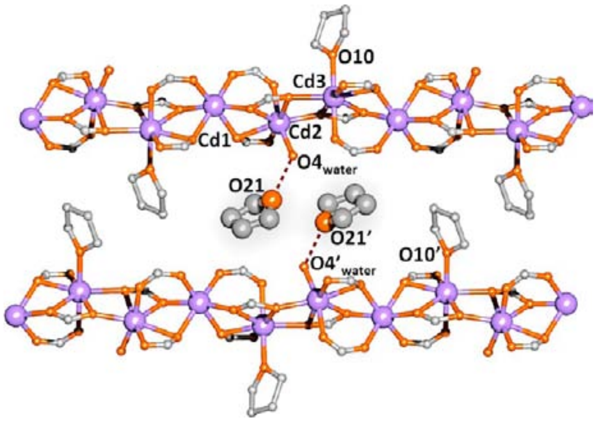

Figure 2. Part of channel A along the *a* axis in **1D** showing coordinated THF to Cd3 and hydrogen bonding between coordinated water and free THF molecule; O21···O4 = 2.553 Å.

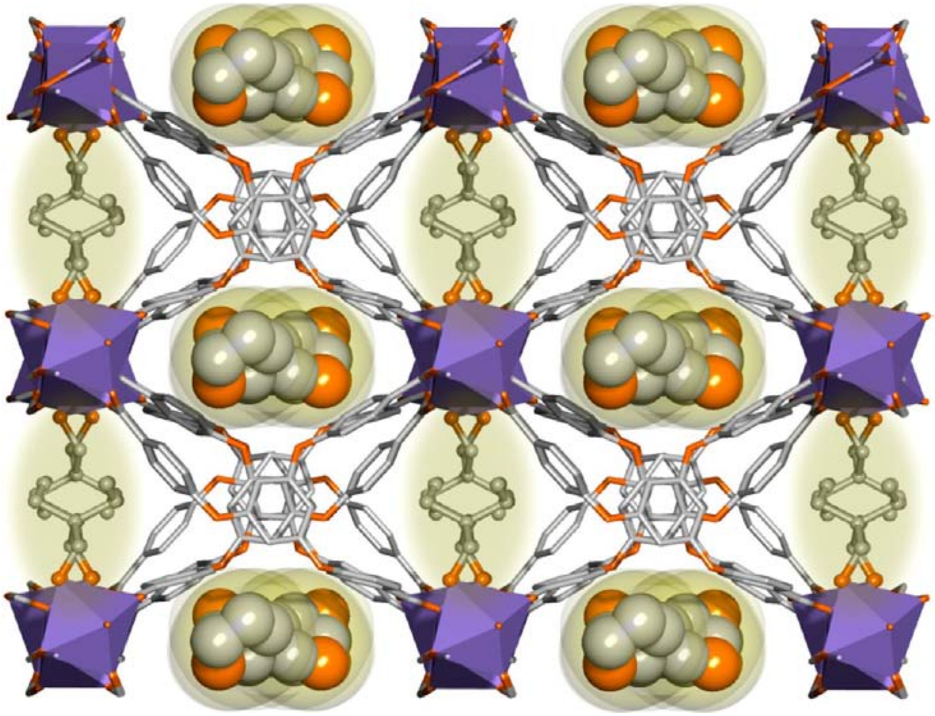

Figure 3. Packing diagram of compound **1$\supset$BuOH** showing biporous functionality with the coordinated BuOH molecules in pore A and free THF guests (space fill) in pore B.

flexible aliphatic straight-chain guest BuOH by the replacement of all coordinated water molecules to give compound **1$\supset$BuOH**. In the case of compound **1$\supset$BuOH**, it was observed that both pores are filled with two different guest molecules; i.e., in pore A, all of the THF guests are replaced by BuOH and then subsequently coordinated to the metal center (Figure 3). Because guest BuOH has a long hydrophobic flexible aliphatic C4 tail, the least reduction in the pore dimensions was observed with a proper fitting of the coordinated BuOH in pore A of **1$\supset$BuOH**. Unexpectedly, pore B is still occupied with the parent THF guest molecules. This specific replacement of guest THF in only pore A may be attributed to the presence of active metal centers in pore A to accommodate BuOH via coordination, which is not possible in pore B, where no free or labile coordination site is present there. Also, the sizes of both pores are different. Pore A (where BuOH is coordinated) has a vertical pore length of 5.113 Å (excluding van der Waals radii), while that of channel B is 3.881 Å in **1$\supset$BuOH**. This type of adjustment of the pore dimension for self-sorting of the guest molecule is unprecedented,[40] which is possible because of the cooperative actions of the soft inorganic backbone and flexible ligand. Moreover, we could successfully study the single-crystal X-ray structure of the desolvated phase **1H** (H stands for heated) by heating **1$\supset$THF** at 180 °C under vacuum. **1H** showed complete replacement of coordinated water by THF guest molecules, which block the free coordination space, solely resulting in a nonporous material. Partial-to-complete exchange of water by THF may be favored by an increase in the temperature and the proximity of the cadmium center with free THF molecule held by hydrogen bonding with coordinated water molecules. Coordinated THF molecules are found to be disordered in the SC-XRD structure, and hence its presence in the compound was also examined by ^{1}H NMR analysis by digesting the compound (**1H**) in a DCl/D_2O mixture (Figure S19 in the Supporting Information, SI). This is the most squeezed structure among all of the phases generated from the parent compound (Figure 4a). In **1H**, the solvent-accessible void was found to be 10.5% per unit cell, which suggests contraction of the free coordination volume to ~70% compared to the parent compound. Structural changes were prominently observed when the simulated PXRD patterns of all of the

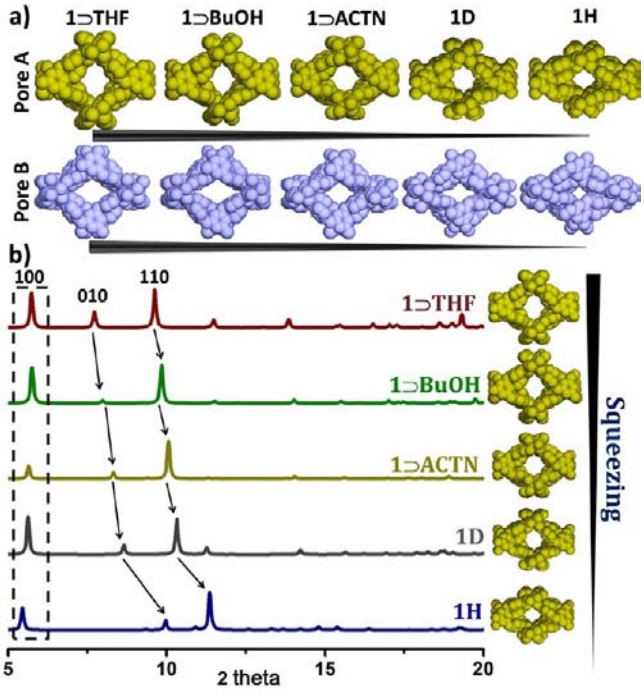

Figure 4. (a) Squeezing of pores A and B for different guest-driven compounds, along with (b) simulated PXRD patterns. In pore A, coordinated guest molecules are omitted for clarity.

Scheme 2. Schematic View Showing Guest-Dependent Two-Way Modulation for Chemical Blocking/Unblocking of the Parent Compound

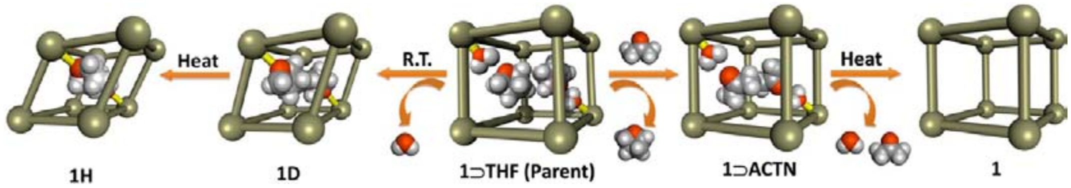

compounds were compared (Figure 4b). The reflection from the [100] plane remains almost constant for all of the phases, and from the most porous compound **1⊃THF** to the most squeezed **1H** compound, a right shift of the [010] and [110] planes was observed (Figure 4b). Among the three guest molecules, i.e., THF, ACTN, and BuOH, guests THF and BuOH are coordinating but have different dimensions. So, drastic guest-dependent differences were observed in their inclusion compounds. We finally focused on two compounds, i.e., **1⊂ACTN** and **1H**, from which we generated two extreme phases (porous and nonporous) to show the effect of guests on modification of the active coordination space and their resulting porous behaviors. TGA of both compounds showed stability of the frameworks up to ~350 °C. To support this phenomenon, gas sorption studies were performed for guest-driven nonporous and porous forms of the parent compound. Compound **1⊃ACTN** and **1D** were subjected to pretreatment under vacuum to get the guest-free forms **1** and **1H**, respectively. TGA of guest-free forms of these two compounds showed no weight loss up to 230 °C and slowly decomposed after that, supported by variable-temperature PXRD studies (Figure S21 and S22 in the SI). Compound **1⊃ACTN** can lose free guest ACTN as well as coordinated water molecules to give the porous phase **1**, where both pores A and B are open. In the case of **1H**, pore A is blocked with a coordinated THF guest and simultaneously pore B is squeezed as well, where THF acts as a blocking coordinating agent in pore A (Scheme 2). It is worth mentioning that guest-dependent two-way modulation to open and closed frameworks was strongly supported by CO_2 sorption at 195 K. Sorption results showed almost negligible uptake of ~1 cm^3/g of CO_2 by **1H**, whereas almost 100 times more uptake was achieved by compound **1** with 104 cm^3/g uptake of CO_2 with a characteristic type I curve (Figure 5). In Scheme 2, it is briefly explained about how pore windows of the framework can be closed and opened upon guest switching inside the coordination space. Compound **1** showed high uptake of CO_2 compared to other gases like N_2, CH_4, and O_2 at 298 K, which is due to good polarizability and a large quadrupole moment of CO_2 molecules, which allows it to interact strongly with the framework and makes it possible to enter into the pore. This clearly indicates that, even though the effective pore size of the framework (5.8 Å, calculated by the Horvath–Kawazoe size distribution curve from CO_2 sorption) is large enough to accommodate all of these gas molecules, electronic interaction plays a role apart from size/shape insights for the selective sorption of CO_2 over other gas molecules.

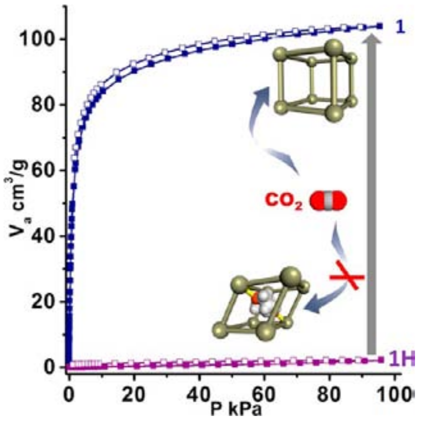

Figure 5. CO_2 sorption isotherms for **1** and **1H** at 195 K.

CONCLUSION

In conclusion, we have shown here guest-dependent structural dynamism of a 3D biporous PCP containing a flexible ligand and an active inorganic backbone. By SCSC structural transformation studies, we have demonstrated controlled chemical blocking and unblocking of active pores of the dynamic framework along with guest-dependent contraction and expansion of the channels with as much as 70% contraction of the void volume. It is also noteworthy that dynamic activities within the active coordination space of the framework are also supported by the almost 100 times increase in carbon dioxide sorption by a controlled porous phase compared to the air-dried nonporous phase. These types of soft materials with porous scaffolds would be useful as intelligent host materials not only for their zeolitic properties but also for their enzyme-like specificity.

ASSOCIATED CONTENT

Ⓢ Supporting Information

X-ray crystallographic data in CIF format, detailed structural analysis, PXRD, SC-XRD data and details, and gas sorption data and details. This material is available free of charge via the Internet at http://pubs.acs.org.

AUTHOR INFORMATION

Corresponding Author

*E-mail: sghosh@iiserpune.ac.in. Phone: +91 20-2590-8076. Fax: +91-20-2590-8186.

Notes

The authors declare no competing financial interest.

ACKNOWLEDGMENTS

We are grateful to IISER Pune for research facilities. DAE (Project 2011/20/37C/06/BRNS) and DST (Project GAP/DST/CHE-12-0083) are acknowledged for financial support. B.J. and S.S.N. are thankful to CSIR for SRF.

REFERENCES

(1) (a) O'Keeffe, M.; Yaghi, O. M. *Chem. Rev.* **2012**, *112*, 675. (b) O'Keeffe, M. *Chem. Soc. Rev.* **2009**, *38*, 1215.

(2) Eddaoudi, M.; Kim, J.; Rosi, N.; Vodak, D.; Wachter, J.; O'Keeffe, M.; Yaghi, O. M. *Science* **2002**, *295*, 469.
(3) Stock, N.; Biswas, S. *Chem. Rev.* **2012**, *112*, 933.
(4) Furukawa, H.; Ko, N.; Go, Y. B.; Aratani, N.; Choi, S. B.; Choi, E.; Yazaydin, A. Ö.; Snurr, R. Q.; O'Keeffe, M.; Kim, J.; Yaghi, O. M. *Science* **2010**, *329*, 424.
(5) Millward, A. R.; Yaghi, O. M. *J. Am. Chem. Soc.* **2005**, *127*, 17998.
(6) Farha, O. K.; Yazaydın, A. O.; Eryazici, I.; Malliakas, C. D.; Hauser, B. G.; Kanatzidis, M. G.; Nguyen, S. T.; Snurr, R. Q.; Hupp, J. T. *Nat. Chem.* **2010**, *2*, 944.
(7) Suh, M. P.; Park, H. J.; Prasad, T. K.; Lim, D.-W. *Chem. Rev.* **2012**, *112*, 782.
(8) Shimomura, S.; Horike, S.; Matsuda, R.; Kitagawa, S. *J. Am. Chem. Soc.* **2007**, *129*, 10990.
(9) Liu, Q.-K.; Ma, J.-P.; Dong, Y.-B. *J. Am. Chem. Soc.* **2010**, *132*, 7005.
(10) Li, J.-R.; Sculley, J.; Zhou, H.-C. *Chem. Rev.* **2012**, *112*, 869.
(11) Lee, J. Y.; Farha, O. K.; Roberts, J.; Scheidt, K. A.; Nguyen, S. T.; Hupp, J. T. *Chem. Soc. Rev.* **2009**, *38*, 1450.
(12) Yoon, M.; Srirambalaji, R.; Kim, K. *Chem. Rev.* **2012**, *112*, 1196.
(13) Horike, S.; Dinca, M.; Tamaki, K.; Long, J. R. *J. Am. Chem. Soc.* **2008**, *130*, 5854.
(14) Song, F.; Wang, C.; Falkowski, J. M.; Ma, L.; Lin, W. *J. Am. Chem. Soc.* **2010**, *132*, 15390.
(15) Chen, B.; Yang, Y.; Zapata, F.; Lin, G.; Qian, G.; Lobkovsky, E. B. *Adv. Mater.* **2007**, *19*, 1693.
(16) Kreno, L. E.; Leong, K.; Farha, O. K.; Allendorf, M.; Duyne, R. P. V.; Hupp, J. T. *Chem. Rev.* **2012**, *112*, 1105.
(17) Lu, Z.-Z.; Zhang, R.; Li, Y.-Z.; Guo, Z.-J.; Zheng, H.-G. *J. Am. Chem. Soc.* **2011**, *133*, 4172.
(18) Nagarkar, S. S.; Joarder, B.; Chaudhari, A. K.; Mukherjee, S.; Ghosh, S. K. *Angew. Chem., Int. Ed.* **2013**, *52*, 2881.
(19) Chen, B.; Wang, L.; Zapata, F.; Qian, G.; Lobkovsky, E. B. *J. Am. Chem. Soc.* **2008**, *130*, 6718.
(20) Zhang, W.; Xiong, R.-G. *Chem. Rev.* **2012**, *112*, 1163.
(21) Sadakiyo, M.; Yamada, T.; Kitagawa, H. *J. Am. Chem. Soc.* **2009**, *131*, 9906.
(22) Liu, Y.; Xuan, W.; Cui, Y. *Adv. Mater.* **2010**, *22*, 4112.
(23) Zhang, W.; Xiong, R.-G. *Chem. Rev.* **2012**, *112*, 1163.
(24) Horcajada, P.; Gref, R.; Baati, T.; Allan, P. K.; Maurin, G.; Couvreur, P.; Ferey, G.; Morris, R. E.; Serre, C. *Chem. Rev.* **2012**, *112*, 1232.
(25) (a) Kitagawa, S.; Kitaura, R.; Noro, S.-i. *Angew. Chem., Int. Ed.* **2004**, *43*, 2334. (b) Vittal, J. J. *Coord. Chem. Rev.* **2007**, *251*, 1781.
(26) Horike, S.; Shimomura, S.; Kitagawa, S. *Nat. Chem.* **2009**, *1*, 695.
(27) (a) Ghosh, S. K.; Zhang, J.-P.; Kitagawa, S. *Angew. Chem., Int. Ed.* **2007**, *46*, 7965. (b) Joarder, B.; Chaudhari, A. K.; Nagarkar, S. S.; Manna, B.; Ghosh, S. K. *Chem.—Eur. J.* **2013**, *19*, 11178−11183. (c) Maji, T. K.; Matsuda, R.; Kitagawa, S. *Nat. Mater.* **2007**, *6*, 142.
(28) Yanai, N.; Kaneko, W.; Yoneda, K.; Ohba, M.; Kitagawa, S. *J. Am. Chem. Soc.* **2007**, *129*, 3496.
(29) Wang, C.; Zhang, T.; Lin, W. *Chem. Rev.* **2012**, *112*, 1084.
(30) (a) Manna, B.; Chaudhari, A. K.; Joarder, B.; Karmakar, A.; Ghosh, S. K. *Angew. Chem., Int. Ed.* **2013**, *52*, 998. (b) Wang, J.-H.; Li, M.; Li, D. *Chem. Sci.* **2013**, *4*, 1793.
(31) Yanai, N.; Kitayama, K.; Hijikata, Y.; Sato, H.; Matsuda, R.; Kubota, Y.; Takata, M.; Mizuno, M.; Uemura, T.; Kitagawa, S. *Nat. Mater.* **2011**, *10*, 787.
(32) Choi, S. B.; Furukawa, H.; Nam, H. J.; Jung, D.-Y.; Jhon, Y. H.; Walton, A.; Book, D.; O'Keeffe, M.; Yaghi, O. M.; Kim, J. *Angew. Chem., Int. Ed.* **2012**, *51*, 8791.
(33) (a) Takaoka, K.; Kawano, M.; Tominaga, M.; Fujita, M. *Angew. Chem., Int. Ed.* **2005**, *44*, 2151. (b) Bradshaw, D.; Warren, J. E.; Rosseinsky, M. J. *Science* **2007**, *315*, 977. (c) Das, M. C.; Bharadwaj, P. K. *J. Am. Chem. Soc.* **2009**, *131*, 10942.
(34) (a) Henke, S.; Schneemann, A.; Wutscher, A.; Fischer, R. A. *J. Am. Chem. Soc.* **2012**, *134*, 9464. (b) Hong, D. H.; Suh, M. P. *Chem. Commun.* **2012**, *48*, 9168.
(35) *SAINT Plus*, version 7.03; Bruker AXS Inc.: Madison, WI, 2004.
(36) Sheldrick, G. M. *SHELXTL, Reference Manual*, version 5.1; Bruker AXS Inc.: Madison, WI, 1997.
(37) Sheldrick, G. M. *Acta Crystallogr., Sect. A* **2008**, 112.
(38) Farrugia, L. *WINGX*, version 1.80.05; University of Glasgow: Glasgow, Scotland, 2009.
(39) Spek, A. L. *PLATON, A Multipurpose Crystallographic Tool*; Utrecht University: Utrecht, The Netherlands, 2005.
(40) Ohmori, O.; Kawano, M.; Fujita, M. *Angew. Chem., Int. Ed.* **2005**, *44*, 1962.